A label-free DNA aptamer-based impedance biosensor for the detection of *E. coli*

Raquel B. Queirós, N. de-los-Santos-Alvarez, J.P. Noronha, M.G.F. Sales

A B S T R A C T

A label-free DNA aptamer-based impedance biosensor for the detection of *E. coli* outer membrane proteins (OMPs) was developed. Two single stranded DNA sequences were tested as recognition elements and compared. The aptamer capture probes were immobilized, with and without 6-mercapto-1-hexanol (MCH) on a gold electrode. Each step of the modification process was characterized by Faradaic impedance spectroscopy (FIS). A linear relationship between the electron-transfer resistance (R_{et}) and *E. coli* OMPs concentration was demonstrated in a dynamic detection range of 1×10^{-7}–2×10^{-6} M. Moreover, the aptasensor showed selectivity despite the presence of other possible water contaminates and could be regenerated under low pH condition. The developed biosensor shows great potential to be incorporated in a biochip and used for *in situ* detection of *E. coli* OMPs in water samples.

Keywords:
DNA, Aptamer
E. coli, OMPs, Biosensor, Faradaic impedance spectroscopy

1. Introduction

Escherichia coli (E. coli) is a bacterium that is commonly found in the gut of humans and other warm-blooded animals. While most strains are harmless, some of them can cause severe food-borne disease such as the *E. coli* O104:H4 outbreak in Germany in 2011. Infections caused by *E. coli* are usually transmitted through consumption of contaminated water or food, such as undercooked meat products and milk. The consumption of contaminated water can cause large and sometimes widely dispersed outbreaks. Symptoms of disease include abdominal cramps, fever, vomiting and diarrhea, which may be bloody in the case of contamination by enterotoxic *E. coli* (ETEC) or enterohemorragic *E. coli* (EHEC). Most patients recover within 10 days, although in a few cases the disease might become life-threatening [1,2]. The routine detection methods for these microorganisms are based on colony forming units (CFU) counting requiring selective culture, and biochemical and serological characterizations. Regardless these methods are sensitive and selective, they need a lot of time to get a result. Besides, these methods are costly and time consuming [3]. The rapid evolution of the symptoms requires a rapid, sensitive and reliable monitoring of bacterial contamination. Biosensors can assume this role in this case [4,5], which in combination with electrochemical techniques for transduction of protein recognition can provide the simplicity and speed required.

Antibodies are the molecular recognition element commonly chosen but they present some limitations such as limited shelf life, thermal and chemical instability leading to denaturation of proteins and loss of binding ability, and target restriction to immunogenic molecules that do not represent constituents of the body [5,6].

As an alternative, aptamers (APTs) are oligonucleotides, DNA or RNA molecules, which can interact with high specificity and affinity to their targets [7,8], due to its ability to fold into numerous tertiary conformations.

Aptamers can be generated by a combinatorial procedure called "systematic evolution of ligands by exponential enrichment" (SELEX) [9] and synthesized in a large quantity *in vitro* in a very reproducible way [10,11]. Several aptamers have been developed to bind different targets, like proteins, small molecules, cells, antibiotics, and viruses [10], in various types of biodetection approaches from label-free [12] to self-reporting or labeling strategies [13] using a variety of assay formats [14].

Evolution of aptamers against bacteria is an underexplored area. Unlike conventional SELEX, the specific target is not usually known and a pool of aptamers against different targets is often found. This obliges to carry out further experiments in order to know the exact nature of the final target if desired. To avoid this cumbersome step,

genetically modified bacteria to overexpress a certain protein is an alternative strategy to bias the selection of aptamers against that specific protein [15].

To the best of our knowledge, five aptamers have been raised against *E. coli.* Three of them are RNA molecules against release factor 1 [16], an O157:H7 specific lipopolysaccharide [17] and an unidentified target [18]. The latter was used in a reverse transcription PCR amplified immunomagnetic sandwich assay as a detection recognition element [19] and a real-time potentiometric assay [20]. However, RNA must be handled with extreme care to prevent the attack of ubiquitous endonucleases that degrade it in a few minutes.

Bruno et al. have recently evolved two DNA aptamers; one against *E. coli* O111 lipopolysaccharides [21] that were employed in a displacement voltammetric assay [22] and the other against outer membrane proteins (OMPs) [23]. In the latter work several aptamers were obtained and tested for competitive displacement FRET assays. The present work describes the use of two of these *E. coli* DNA aptamers (herein called ECA I and II) for the determination of *E. coli* OMPs in waters by the direct identification of OMPs electrochemically.

The electrochemical approach is cost-effective because it does not require expensive instrumentation [24,25] and would allow portability [26]. FIS transduction is especially well suited to detect changes that occur in the solution-electrode interface without the need of labels. This technique was one of the first used for electrochemical transduction of the aptamer–ligand recognition event for small molecules [27], where the associated conformational change can be too small to cause a significant variation in a physical property of appropriate labels such as the case of antibiotics [28,29]. But it can also be used for the detection of large molecules [30–32] or whole cells [33]. The analytical signal, the electron transfer resistance (R_{et}) of a redox probe, is related to the amount of protein bound to the aptamer immobilized on the electrode surface, which correlates with the concentration of proteins present in the sample.

Two DNA aptamer candidate sequences raised against *E. coli* OMPs containing 36 and 37 nucleotides were tested [23]. Both DNA sequences were also immobilized with and without the 6-mercapto-1-hexanol (MCH) to study if the nonspecific effects are reduced with the application of a bilayer. The sensor interface plays a crucial role in the overall performance of electrochemical sensors. Nonspecific adsorption effects can be reduced by employing mixed self-assembled monolayers (SAMs) containing a thiol-derivatized capture probe DNA and a spacer thiol, mainly MCH [34].

APT-based FIS biosensors could be a good alternative for the rapid, sensitive, and specific detection of *E. coli* species in environmental samples.

2. Materials and methods

2.1. Apparatus

All electrochemical measurements were performed with a standard three electrode cell controlled by an Autolab PGstat-12 potentiostat with NOVA software (EcoChemie, The Netherlands).

A (0.5 mm diameter) platinum wire acted as an auxiliary electrode and a (1.6 mm diameter) gold electrode as a working electrode (Bioanalytical Systems, Inc, IN). The reference electrode used was an Ag|AgCl|KCl saturated reference electrode from Crison Instrument, SA.

2.2. Reagents and solutions

A lawn of E. coli ATCC® 8739™ (USA). *E. coli* OMPs were extracted according to Ref. [23]. 5′-SH-GTC TGC GAG CGG GGC GCG GGC CCG GCG GGG GAT GCG C-3′ (ECA I) and 5′-SH-ACG GCG CTC CCA ACA GGC CTC TCC TTA CGG CAT ATT A-3′ (ECA II) aptamers were purchased from Sigma–Aldrich (Spain). The thiol-modified aptamers were commercially supplied as the respective disulfides. Prior to use, these products were treated with dithiothreitol (DTT, Sigma) and then purified by elution through a DNA gel filtration Ilustra NAP 25 columns with Sephadex G25 DNA grade used for DNA purification (GE Healthcare) with double-deionized RNAse free water 0.03 μS at 25 °C from ATS (Portugal). Potassium hexacyanoferrate II and potassium hexacyanoferrate III were purchased from Sigma–Aldrich and Panreac, respectively. Hexaammineruthenium(III) chloride and MCH were purchased from Aldrich. Salts for buffer solutions were prepared in double-deionized RNAse free water (DD) 0.03 μS at 25 °C from ATS (Portugal). Magnesium chloride was purchased from Riedel-del-Häen (Germany), potassium chloride from Merck (Germany), sodium chloride and (tris(hydroxymethyl)aminomethane (TRIS) were obtained from Panreac, and SSPE buffer 20× concentrate (1× = 0.150 M sodium chloride, 0.010 M sodium phosphate, 0.001 M EDTA) and bovine serum albumin (BSA) were obtained from Sigma.

The buffers used in this work were: extraction buffer: phosphate buffer solution; immobilization buffer: 2 × SSPE, (diluted from 20× SSPE); affinity buffer (50 mM TRIS/HCl pH 7.4, 250 mM NaCl, 5 mM $MgCl_2$) and measurement buffer (10 mM TRIS/HCl pH 7.4, 100 mM KCl, 5 mM $[Fe(CN)_6]^{3-/4-}$). Alumina slurries were prepared with MicroPolish deagglomerated alumina powders (1, 0.3, and 0.05 μm) purchased in Buehler (Germany). All the reagents were of analytical grade.

2.3. Experimental methods

2.3.1. Extraction and determination of OMPs concentration

A lawn of *E. coli* ATCC® 8739™ (Crooks strain) (USA) was grown on a blood agar plate overnight at 37 °C. Bacteria were washed from the plate with the extraction buffer and transferred to 10 ml of cold 1.5 M $MgCl_2$ in sterile nuclease-free water. The suspension of bacteria was left overnight at 4 °C to allow the chaotropic action of $MgCl_2$ to extract OMPs. The resultant pellet was washed again with buffer and centrifuged. The liquid was collected and the final concentration of OMPs was estimated spectrophotometrically at 280 nm [23].

2.3.2. Electrode cleaning and pretreatment

The gold electrode was immersed in piranha solution ($3H_2SO_4$:$1H_2O_2$) for 10 min (warning: piranha solution is strongly oxidizing and should be handled with care!). Then the electrode was polished in a cotton cloth sequentially with 1, 0.3 and 0.05 μm alumina slurries. After sonication in an ultrasound bath for 5 min, it was immersed in a 2 M KOH for 1 h at 60 °C. Then the electrode was immersed in concentrated acids at room temperature for 10 min first in H_2SO_4 and after in HNO_3. Finally, the electrode was subjected to several potential cycles between 0 and 1.6 V in 0.1 M H_2SO_4 at 100 mV s^{-1} until a stable background was obtained. The electrodes were rinsed with DD water between each step.

2.3.3. Aptamer immobilization and quantification

Each aptamer was immobilized onto a freshly cleaned electrode overnight. Unless otherwise stated, the electrode was immersed in 2×10^{-8} M ECA I or ECA II in the immobilization buffer at 4 °C. After probe immobilization, the electrode surface was rinsed with DD water to remove the weakly adsorbed aptamer. When preparing SAMs, the aptamer-modified electrode was subsequently immersed in 4.5 mM MCH in the same immobilization buffer for 30 min under stirring, in the dark, and then, rinsed with DD water.

The surface density of immobilized aptamer was determined by chronocoulometric measurements using $[Ru(NH_3)_6]^{3+}$ as previously reported [34].

2.3.4. FIS measurements

The electrodes modified with single (ECA) and mixed (ECA–MCH) SAMs were incubated in varying concentrations of OMPs in the affinity buffer for 90 min, and after a brief washing step with water, they were transferred to the measurement solution to record the impedance spectrum at a bias potential of +0.225 V with a frequency range ranging from 0.1 to 10,000 Hz and an alternating current amplitude of 5 mV.

After measurement, the modified electrodes were washed with a 2 M HCl solution for 20 min, to regenerate the probe for re-use of the modified electrode.

A schematic illustration of the modified electrode with the immobilized capture probes and the detection of the *E. coli* OMPs are presented in Fig. 1.

3. Results

3.1. The principle of ECA impedimetric biosensor

The detailed principle of ECA impedimetric biosensor is illustrated in Fig. 1. Firstly, the aptamer functionalized with a thiol group at its 5′ end was covalently attached on the Au surface. The modified electrode was then blocked with MCH to form a mixed SAM in order to effectively prevent the nonspecific adsorption of OMPs on the electrode surface and also to align the aptamers to facilitate their interaction with the ligand, the OMPs.

In the absence of OMPs, the added redox probe (ferrocyanide/ferricyanide) molecules can exchange electrons with the modified electrode surface but a certain resistance is observed. In the presence of OMPs, the ECA folds around the proteins and forms an OMPs–ECA complex. The formation of this complex blocks the electron transfer and consequently the R_{et} increases.

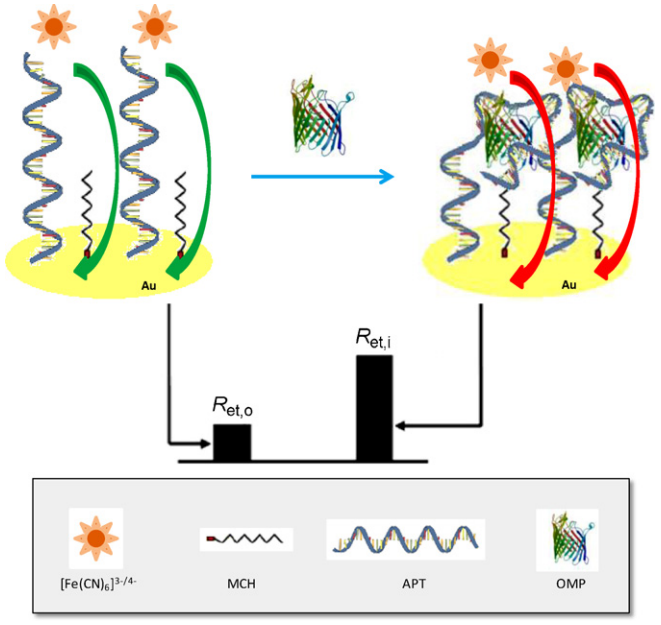

Fig. 1. Schematic illustration of the modified electrodes and the detection of *E. coli* OMPs.

In Fig. 2, the variation of analytical signal expressed as $(R_{et,1}-R_{et,0})/(R_{et,0})$, where $R_{et,1}$ is the R_{et} after incubation for a certain time and $R_{et,0}$ is the R_{et} before incubation with OMPs (R_{et} for the sensing phase) with incubation time is shown. The analytical signal increases rapidly with the increment of incubation time up to 90 min, and then gradually reaches a plateau, indicating that the affinity reaction reaches the equilibrium. Therefore, for further experiments 90 min of incubation time was used.

Ultraviolet–visible (UV–vis) absorption method [35] was used to prove the interaction between APTs and proteins. Fig. 3 shows

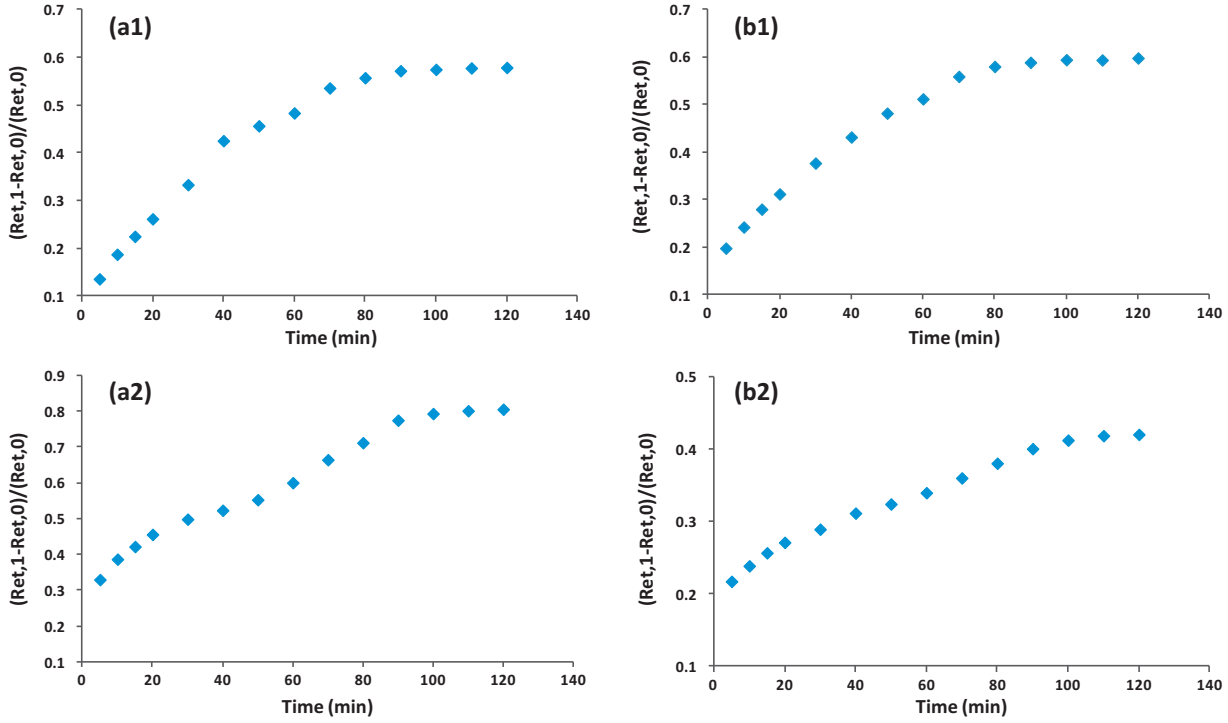

Fig. 2. Variation of analytical signal, expressed as $(R_{et,1}-R_{et,0})/(R_{et,0})$, with incubation time for a concentration of 2×10^{-8} M of OMPs using a SAM prepared from (a1) 2×10^{-8} M ECA I; (a2) 2×10^{-8} M ECA I–MCH; (b1) 2×10^{-8} M ECA II; (b2) 2×10^{-8} M ECA II–MCH.

Table 1
Regression parameters for the 4 different SAMs (ECA I, ECA I–MCH, ECA II and ECA II–MCH) evaluated.

	ECA I	ECA I–MCH	ECA II	ECA II–MCH
Regression equation	$(R_{et,1}-R_{et,0})(\Omega)/(R_{et,0})(\Omega)$ $=(6.22\pm0.07)$ $\log([OMP]/M)+(50.9\pm0.4)$	$(R_{et,1}-R_{et,0})(\Omega)/(R_{et,0})(\Omega)$ $=(5.89\pm0.02)\times10^5[OMP]/M$ $+(0.016\pm0.002)$	$(R_{et,1}-R_{et,0})$ $(\Omega)/(R_{et,0})(\Omega)=(4.6\pm0.1)$ $\log([OMP]/M]+(34.5\pm0.7)$	$(R_{et,1}-R_{et,0})(\Omega)/(R_{et,0})(\Omega)$ $=(9.38\pm0.09)\times10^5$ $[OMP]/M+(0.18\pm0.01)$
r^2	0.9998	0.9999	0.9990	0.9998

absorption spectra of 2×10^{-8} M of aptamers, 3×10^{-7} M of OMPs and the mixture of both (ECA–OMPs) after 60 and 90 min; (a) for ECA I and in (b) for ECA II. Both DNA capture probes (ECA I and ECA II) presented a peak at 260 nm. After the interaction of OMPs with the ECA, is observed that the DNA peak at 260 nm shifts to about 250 nm and expands. Moreover, the peak decreases slightly in terms of absorbance. In (b) the expansion of ECA peaks is broader and there is a greater decrease of absorbance. However in (a) a more reliable behavior is observed in terms of the interaction ECA–OMPs due to the decrease of absorbance along the time. This observed behavior can be an evidence that aptamer wraps around OMPs.

The amount of aptamer chemisorbed onto the Au electrode was estimated by chronocoulometry in SAMs prepared from 2×10^{-8} M aptamer solutions. A value of $(9.07\pm0.03)\times10^{11}$ molecule cm^{-2} was obtained when ECA I was the only component of the SAM. After immersion in MCH solutions for 1 h, the amount of ECA I diminished to $(3.05\pm0.04)\times10^{11}$ molecule cm^{-2}, which is in good agreement with the well-known displacement effect of MCH on previously formed SAMs when used at mM concentrations. Higher concentrations of aptamer solutions up to 2×10^{-7} M did not increase the amount of aptamer attached onto the Au surface $(9.06\pm0.03)\times10^{11}$ molecule cm^{-2} and $(2.80\pm0.04)\times10^{11}$ molecule cm^{-2} for single and mixed monolayers, respectively), so a concentration of 2×10^{-8} M was selected for further experiments. Equivalent values were estimated from ECA II and ECA II–MCH monolayers.

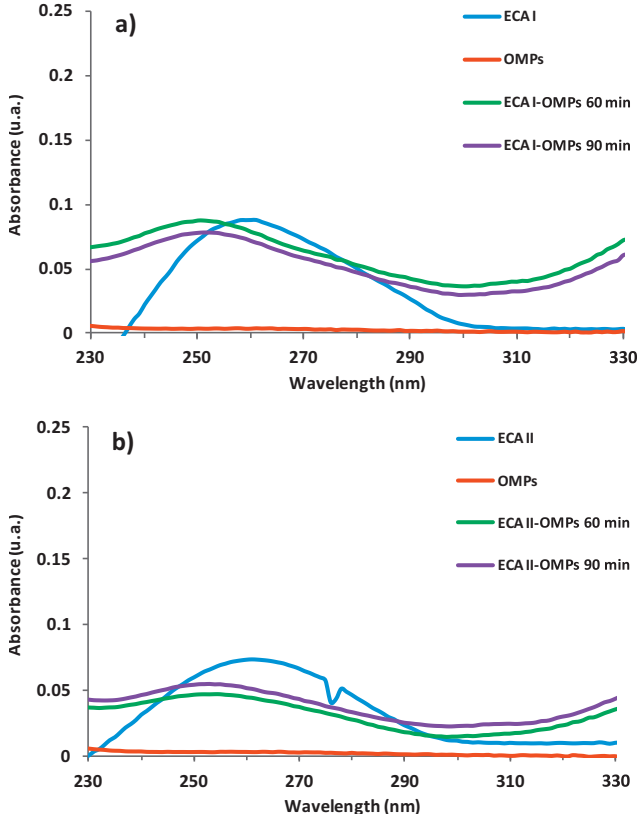

Fig. 3. UV spectra of the 2×10^{-8} M aptamers, 3×10^{-7} M OMPs and the interaction between them along time (a) for ECA I, and (b) for ECA II.

3.2. Sensor performance

The ECA I and ECA II capture probes were evaluated by testing the change in electron-transfer behavior before and after binding of OMPs. FIS measurements were conducted at room temperature in the measurement buffer. The experimental Nyquist plots were fitted by the electrochemical circle fit of NOVA 1.6 software using an electronic circuit based on the Randles theoretical model [36]. This equivalent circuit includes the ohmic resistance of the electrolyte solution, R_s, the Warburg impedance, Z_w, resulting from the diffusion of the redox-probe, the double-layer capacitance, C_{dl}, and the electron-transfer resistance, R_{et}. The latter two components, C_{dl} and R_{et}, represent interfacial properties of the electrode, which are highly sensitive to the surface modification. When a non-homogeneous surface layer exists, a constant phase element (CPE, $CPE=A^{-1}(j\omega)^{-n}$) can be introduced into the circuit instead of a capacitance. The CPE becomes equal to the C_{dl} when $n=1$. The experimental electrochemical impedance spectra can be well fitted with equivalent electronic circuit ($R_s(CPE[R_{et}Z_w])$) including R_s, Z_w, CPE and R_{et}, see Table S1 and Figure S1 from supplementary data.

The bare Au electrode exhibits a very small semicircle domain, indicating a very low electron-transfer resistance as expected (Fig. 4). The self-assembly of the ECA onto the electrode surface increases R_{et} in good agreement with the electrostatic repulsion between negative charges of the DNA aptamer backbone and the redox probe, $[Fe(CN)_6]^{3-/4-}$, which results in a barrier for the interfacial electron transfer. In mixed SAMs, after the immobilization of MCH layer, a decrease tendency of R_{et} is observed due to the displacement of some aptamers from the surface of the gold electrode, as indicated above. Subsequently, the incubation of ECA with OMPs of concentrations between 1×10^{-7} and 2×10^{-6} M in affinity buffer progressively increases R_{et} in the four modified surfaces tested because OMPs inhibit charge transfer between redox probe and the Au electrode. As shown in Table 1, there is a linear relationship between the normalized R_{et} and the target concentration in the range of 1×10^{-7} and 2×10^{-6} M for mixed SAMs. However, the interaction of ECA I and ECA II simple SAMs, with OMPs, presented a linear dependency with the logarithm of the OMPs concentration. This difference in behavior is not due to unspecific adsorption on Au electrode. BSA was used as a control experiment. In all cases the incubation in increasing concentrations of BSA did not lead to a concentration-dependent increase in R_{et}. On the contrary, the R_{et} remained almost constant with BSA concentration.

3.3. Cross-reactivity to other molecules

To assess the nonspecific binding of other molecules that could be present in water systems the different SAMs were incubated with 2×10^{-6} M OMPs, with 1 nM of Microcystin–Leucine, Arginine (MCYST–LR) and with a mixture of both for 90 minutes in the affinity buffer. This MCYST–LR concentration is the recommended maximum level of MCYST–LR in waters established by Ref. [37]. The electron-transfer resistance of the complexes ECA I–OMPs and ECA II–OMPs for both types of sensing phases (single or

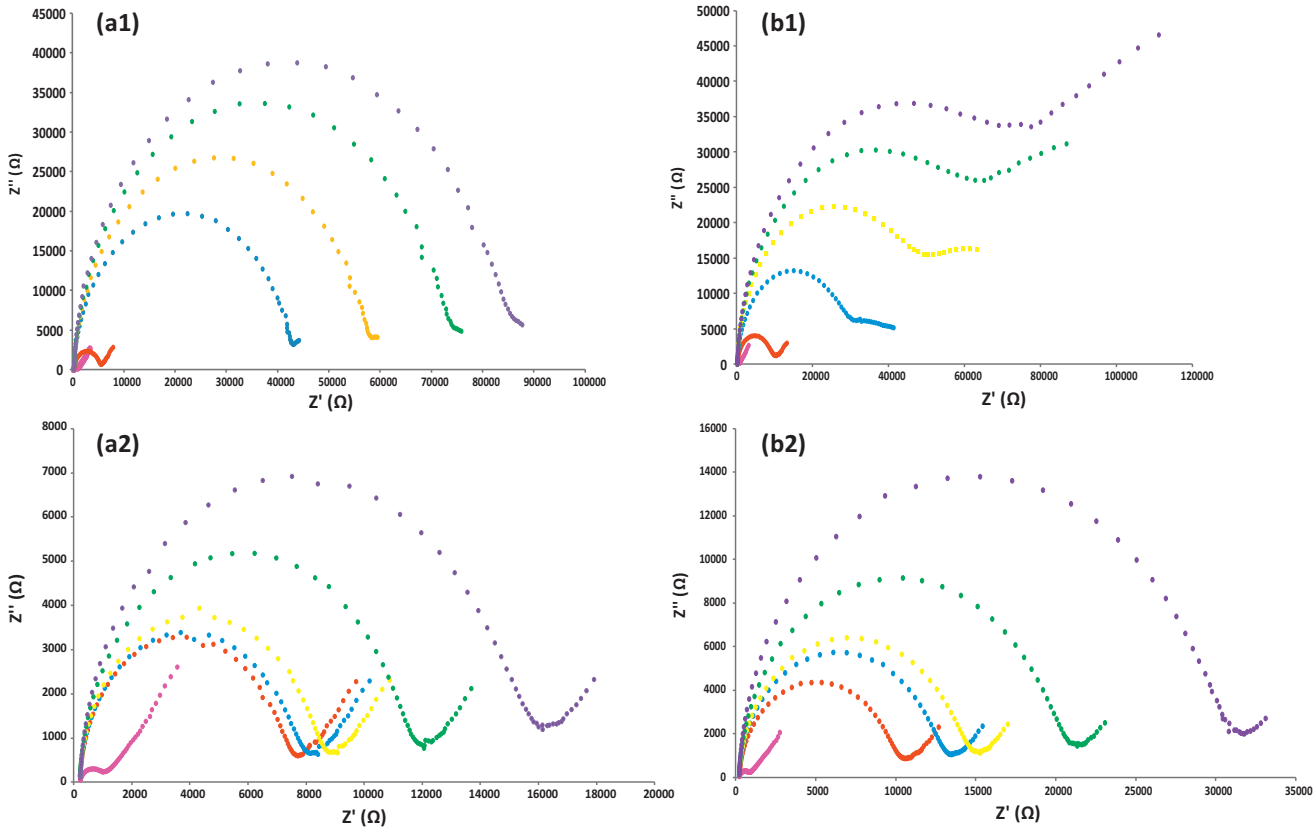

Fig. 4. Nyquist plots of the modified electrodes with single ECA I (a1) and ECA II (b1) and mixed ECA I–MCH (a2) and ECA II–MCH (b2) SAMs. All steps of the detection system were recorded and displayed, (magenta) clean bare gold electrode, (red) after ECA immobilization in simple SAMs or after ECA–MCH immobilization in mixed SAMs, and after interaction with (blue) 1×10^{-7} M, (yellow) 3×10^{-7} M, (green) 9×10^{-7} M and (purple) 2×10^{-6} M *E. coli* OMPs. See Section 2.3 for conditions details.

mixed monolayers) presented a much higher value than after incubating in MCYST–LR solution (Fig. 5). In the case of the mixture OMPs–MCYST–LR the R_{et} presented a similar value to the complexes ECA I–OMPs and ECA II–OMPS. These results showed the specificity of OMPs binding to the aptamer on the electrode even in the presence of potential interferences, and that FIS successfully detected this binding event.

3.4. Regeneration of sensing phase

The regeneration of the sensing phase was tested by carrying out consecutive binding and washing steps. First, impedimetric measurements of the clean Au electrode surface, aptamer capture probe and bound *E. coli* OMPs (2×10^{-6} M) were performed. Then, several regeneration solutions (urea, TRIS–HCl–NaCl, glycine, HNO_3, HCl and tween 20) were used to regenerate the sensing phase. Although the signal decreased in some cases, it did not reach the baseline level and only HCl at 2 M presented a suitable result. As can be seen in Fig. 6, for single SAMs, ECA I and ECA II, the surface is entirely regenerated after 20 min and capable of detecting OMPs again with the same sensitivity. In the case of mixed SAMs, ECA I–MCH and ECA II–MCH the regeneration is not as effective, presenting a regeneration of about 15% and 45%, respectively. Even though, these capture probes are also capable of detecting OMPs in a second binding event, indicating that the biosensor has good stability and regeneration.

3.5. Detection of E. coli OMPs in environmental water samples

In order to investigate the application of the present method to the analysis of environmental waters (pH 6.5), spiked waters were tested and the corresponding relative errors calculated.

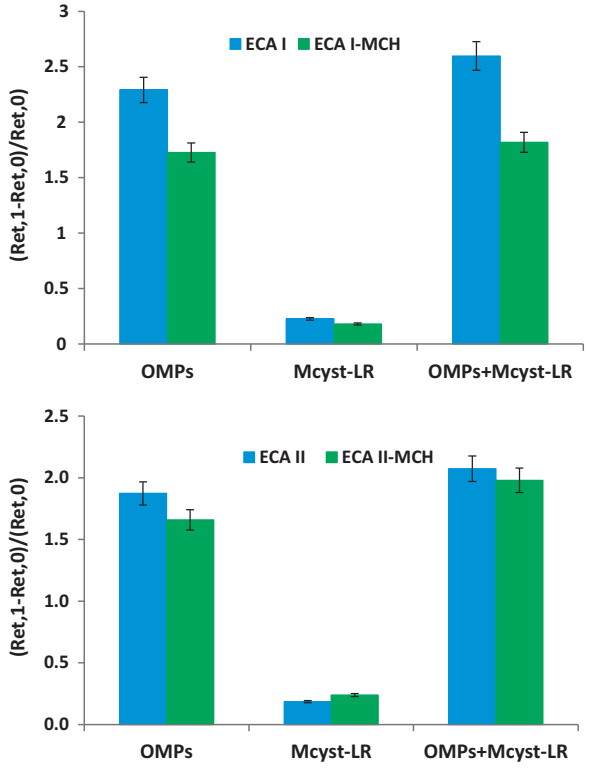

Fig. 5. Binding specificity of aptamers to its protein target (OMPs). Variation of the analytical signal, expressed as $(R_{et,1} - R_{et,0})/(R_{et,0})$, using single (ECA) or mixed (ECA–MCH) monolayers upon exposure to 2×10^{-6} M OMPs, 1×10^{-9} M Microcystin–LR (MCYST–LR), and the mixture of both. Upper panel: ECA I, lower panel: ECA II.

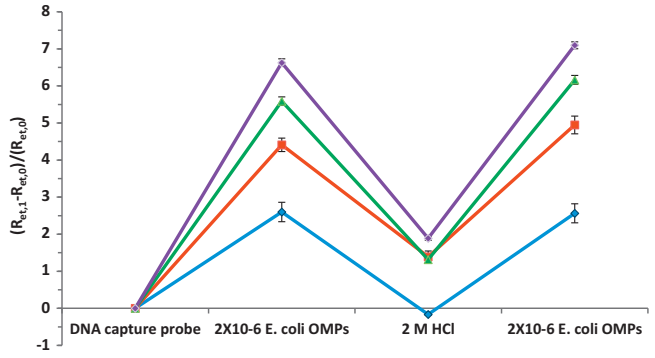

Fig. 6. $(R_{et,1}-R_{et,0})/(R_{et,0})$ values for the several steps of binding and regeneration for (blue) ECA I, (red) ECA I–MCH, (green) ECA II, and (purple) ECA II–MCH sensing phases studied.

Environmental water samples were collected in an artesian well and stored in amber glass bottles previously rinsed with double-deionized RNAse free water. The pH and ionic strength of the water samples were adjusted by addition of affinity buffer (50:50), and they were stored at 4 °C until analysis. *E. coli* bacteria were cultured in blood agar; thereafter the membrane of cells was destroyed and proteins extracted, according to Section 2.3.1. After quantifying the concentration of OMPs by UV at 280 nm, environmental water samples were doped with these proteins solution for the final concentrations of 2.00, 5.00 and 7.00 ($\times 10^{-7}$ M). *E. coli* OMPs is achieved. These assays were carried out with sensors calibrated within 1×10^{-7} to 2×10^{-6} M of *E. coli* OMPs. The average recoveries of three spiked solutions for ECA I, ECA I–MCH, ECA II and ECA II–MCH were 80.2%, 88.8%, 85.6% and 138.9%, respectively and thus confirming the accuracy of the analytical data. Thus, this biosensor held promise as a fast and viable technique for *E. coli* detection in real samples without the need for long cultures.

4. Conclusions

A signal-on electrochemical aptasensor for the detection of *E. coli* OMPs based on the specific recognition between an immobilized aptamer capture probe onto a gold electrode and bacterial proteins, using the couple ferricyanide/ferrocyanide as a redox probe for FIS measurements is proposed. In general terms, both single and mixed monolayers showed a concentration-dependence behavior. Single aptamer monolayers presented higher affinity for OMPs than mixed ones in terms of electron transfer resistance variation. Furthermore, this type of sensing phase was almost completely regenerated (under low pH conditions) and the deviation of the subsequent detection was less than 5%.

These analytical features, as well as its fabrication easiness and operational convenience, make it a promising method to be involved into biochip fabrication allowing the decentralized detection of *E. coli* (further from large lab facilities).

With the identification of new aptamer structures for specific bacterial targets, the aptamer-based biosensor approach may find its place in the market to favorably compete with the rather expensive antibody/antigen methods, which is the main commercial rapid method used at the present time.

Acknowledgments

Raquel B. Queirós thanks FCT, *Fundação para a Ciência e Tecnologia*, for the PhD grant SFRH/BD/49072/2008. Raquel B. Queirós also thanks Dr. Marcos García Ocaña from the biology and cellular cultures unit (Universidad de Oviedo) for his help in the cultivation and extraction of proteins from *E. coli* cells. N. de-los-Santos-Álvarez thanks Spanish Government for a Ramón y Cajal contract. This work was financed by project CTQ2008-02429 granted to "Grupos Consolidados" and the European Regional Development Fund.

Appendix A. Supplementary data

Supplementary data associated with this article can be found, in the online version, at http://dx.doi.org/10.1016/j.snb.2013.01.062.

References

[1] World Health Organization (WHO), Prevention and Control of Enterohaemorrhagic *Escherichia coli* (EHEC) Infections, Report of a Consultation, Geneva, Switzerland, 1997.
[2] World Health Organization (WHO), New frontiers in the development of vaccines against enterotoxinogenic (ETEC) and enterohaemorrhagic (EHEC) *E. coli* infections-Part II. Weekly Epidemiological Record, 74 (1999) 105–112.
[3] C. Ercole, M. Del Gallo, L. Mosiello, S. Baccella, A. Lepidi, *Escherichia coli* detection in vegetable food by a potentiometric biosensor, Sensors and Actuators B91 (2003) 163–168.
[4] A.P.F. Turner, Biosensors sense and sensitivity, Science 290 (2000) 1315–1317.
[5] X. Li, L. Shen, D. Zhang, H. Qi, Q. Gao, F. Ma, C. Zhang, Electrochemical impedance spectroscopy for study of aptamer–thrombin interfacial interactions, Biosensors and Bioelectronics 23 (2008) 1624–1630.
[6] C.K. O'Sullivan, Aptasensors the future of biosensing, Analytical and Bioanalytical Chemistry 372 (2002) 44–48.
[7] A.D. Ellington, J.W. Szostak, In vitro selection of RNA molecules that bind specific ligands, Nature 346 (1990) 818–822.
[8] S. Tombelli, M. Minunni, M. Mascini, Analytical applications of aptamers, Biosensors and Bioelectronics 20 (2005) 2424–2434.
[9] C. Tuerk, L. Gold, Systematic evolution of ligands by exponential enrichment: RNA ligands to bacteriophage T4 DNA polymerase, Science 249 (1990) 505–510.
[10] R. Stoltenburg, C. Reinemann, B. Strehlitz, SELEX—A (r)evolutionary method to generate high-affinity nucleic acid ligands, Biomolecular Engineering 24 (2007) 381–403.
[11] W. Mok, Y. Li, Recent progress in nucleic acid aptamer-based biosensors and bioassays, Sensors 8 (2008) 7050–7084.
[12] N. de-los-Santos-Álvarez, M.J. Lobo-Castañón, A.J. Miranda-Ordieres, P. Tuñón-Blanco, Aptamers as recognition elements for label-free analytical devices, TrAC 27 (5) (2008) 437–446.
[13] R. Miranda-Castro, N. de-los-Santos-Álvarez, M.J. Lobo-Castañón, A.J. Miranda-Ordieres, P. Tuñón-Blanco, Structured nucleic acid probes for electrochemical devices, Electroanalysis 21 (19) (2009) 2077–2090.
[14] M. Mascini, I. Palchetti, S. Tombelli, Nucleic acid peptide aptamers: fundamentals bioanalytical aspects, Angewandte Chemie International Edition 51 (2012) 1316–1332.
[15] E. Torres-Chavolla, E.C. Alocilja, Aptasensors for detection of microbial and viral pathogens, Biosensors and Bioelectronics 24 (11) (2009) 3175–3182.
[16] S. Sando, A. Ogawa, T. Nishi, M. Hayami, Y. Aoyama, In vitro selection of RNA aptamer against *Escherichia coli* release factor 1, Bioorganic and Medicinal Chemistry Letters 17 (5) (2007) 1216–1220.
[17] Y.J. Lee, S.R. Han, J.S. Maeng, Y.J. Cho, S.W. Lee, In vitro selection of *Escherichia coli* O157:H7-specific RNA aptamer, Biochemical and Biophysical Research Communications 417 (1) (2012) 414–420.
[18] H.M. So, D.W. Park, E.K. Jeon, Y.H. Kim, B.S. Kim, C.K. Lee, S.Y. Choi, S.C. Kim, H. Chang, J.O. Lee, Detection and titer estimation of *Escherichia coli* using aptamer-functionalized single-walled carbon-nanotube field-effect transistors, Small 4 (2) (2008) 197–201.
[19] H.J. Lee, B.C. Kim, K.W. Kim, Y.K. Kim, J. Kim, M.K. Oh, A sensitive method to detect *Escherichia coli* based on immunomagnetic separation and real-time PCR amplification of aptamers, Biosensors and Bioelectronics 24 (12) (2009) 3550–3555.
[20] G.A. Zelada-Guillen, S.V. Bhosale, J. Riu, F.X. Rius, Real-time potentiometric detection of bacteria in complex samples, Analytical Chemistry 82 (22) (2010) 9254–9260.
[21] J.G. Bruno, M.P. Carrillo, T. Phillips, In vitro antibacterial effects of antilipopolysaccharide DNA aptamer-C1qrs complexes, Folia Microbiologica 53 (4) (2008) 295–302.
[22] C. Luo, Y. Lei, L. Yan, T. Yu, Q. Li, D. Zhang, S. Ding, H. Ju, A. Rapid, Sensitive aptamer-based electrochemical biosensor for direct detection of *Escherichia coli* O111, Electroanalysis 24 (5) (2012) 1186–1191.
[23] J.G. Bruno, M.P. Carrillo, T. Phillips, C.J. Andrews, Journal of Fluorescence 20 (2010) 1211–1223.
[24] M. Dijksma, B. Kamp, J.C. Hoogvliet, W.P. Van Bennekom, Development of an electrochemical immunosensor for direct detection of interferon-γ at the attomolar level, Analytical Chemistry 73 (2001) 901–907.
[25] Y.S. Kim, H.S. Jung, T. Matsuura, H.Y. Lee, T. Kawai, M.B. Gua, Electrochemical detection of 17β-estradiol using DNA aptamer immobilized gold electrode chip, Biosensors and Bioelectronics 22 (2007) 2525–2531.
[26] B.V. Dorst, J. Mehta, K. Bekaert, E.R. Martina, W.D. Coen, P. Dubruel, R. Blust, J. Robbens, Recent advances in recognition elements of food and

environmental biosensors: a review, Biosensors and Bioelectronics 26 (2010) 1178–1194.
[27] M. Zayats, Y. Huang, R. Gill, C.A. Ma, I. Willner, Label-Free, Reagentless aptamer-based sensors for small molecules, Journal of the American Chemical Society 128 (2006) 13666–13667.
[28] N. de-los-Santos-Álvarez, M.J. Lobo-Castañón, A.J. Miranda-Ordieres, P. Tuñón-Blanco, Modified-RNA aptamer-based sensor for competitive impedimetric assay of neomycin B, Journal of the American Chemical Society 129 (2007) 3808–3809.
[29] E. González-Fernández, N. de-los-Santos-Álvarez, M.J. Lobo-Castañón, A.J. Miranda-Ordieres, P. Tuñón-Blanco, Aptamer-based inhibition assay for the electrochemical detection of tobramycin using magnetic microparticles, Electroanalysis 23 (2011) 43–49.
[30] M.C. Rodriguez, A.N. Kawde, J. Wang, Aptamer biosensor for label-free impedance spectroscopy detection of proteins based on recognition-induced switching of the surface charge, Chemical Communications 34 (2005) 4267–4269.
[31] F. Rohrbach, H. Karadeniz, A. Erdem, M. Famulok, G. Mayer, Label-free impedimetric aptasensor for lysozyme detection based on carbon nanotube-modified screen-printed electrodes, Analytical Biochemistry 421 (2012) 454–459.
[32] Y. Xu, L. Yang, X.Y. Ye, P.A. He, Y.Z. Fang, An aptamer-based protein biosensor by detecting the amplified impedance signal, Electroanalysis 18 (2006) 1449–1456.
[33] M. Labib, A.S. Zamay, D. Muharemagic, A.V. Chechik, J.C. Bell, M.V. Berezoyski, Aptamer-based viability impedimetric sensor for viruses, Analytical Chemistry 84 (2012) 1813–1816.
[34] A.B. Steel, T.M. Herne, M.J. Tarlov, Electrochemical quantitation of DNA immobilized on gold, Analytical Chemistry 70 (1998) 4670–4677.
[35] M. Jing, M.T. Bowser, Methods for measuring aptamer–protein equilibria: a review, Analytica Chimica Acta 686 (2011) 9–18.
[36] J.E.B. Randles, Kinetics of rapid electrode reactions, Discussions of the Faraday Society 1 (1947) 11–19.
[37] World Health Organization (WHO), Drinking-water quality guidelines for parameters of concern in agricultural drainage water—annex 3, Technical Report, 1998, pp. 281–289.